

# Wireless Electrohydrodynamic Actuators for Propulsion and Positioning of Miniaturized Floating Robots

Hiroki Shigemune,\* Kittamet Pradidarcheep, Yu Kuwajima, Yumeta Seki, Shingo Maeda, and Vito Cacucciolo\*

Autonomous soft robots require compact actuators generating large strokes and high forces. Electro-fluidic actuators are especially promising, they combine the advantages of electroactive polymers (low-power consumption, fast response, and electrical powering) with the versatility of fluidic systems (force/stroke amplification). EHD (electrohydrodynamic) actuators are electro-fluidic actuators whose motion results from charges being induced and accelerated in a liquid. They are extremely compact, silent, and low power ( $\leq 10$  mW). They have been recently demonstrated in stretchable pumps and for the wireless propulsion of simple floating robots. This study demonstrates simultaneous wireless propulsion ( $2.5 \text{ mm s}^{-1}$ ) and control of a 1 cm sized robot using a single DC signal. Voltage is applied between an electrode on the floating robot and a fixed one, both exposed to a dielectric liquid. Results support the underlying physical mechanism as EHD and characterize robot motion with different fluorocarbon liquids and voltages between 400 and 1800 V. Path following is demonstrated with a  $3 \times 3$  array of electrodes. EHD actuators prove to be a simple, compact, low power alternative to magnetic and acoustic actuators for wireless powering and control of miniaturized robots, with applications in precision assembling at the micro/mesoscale, lab-on-chip, tactile displays, and active surfaces.

combining the advantages of electroactive polymers (EAPs) with the ones of hydraulic/pneumatic systems. A number of different physical mechanisms and actuators architectures have been reported in the last decade, in particular for powering soft robots. HASELs and HAXELs replace the dielectric elastomer in dielectric elastomer actuators with a dielectric liquid.<sup>[1,2]</sup> Electro-ribbons make use of a liquid meniscus to amplify the electrical forces required for zipping.<sup>[3]</sup> Electrohydrodynamic (EHD) stretchable pumps transfer electrical energy into a continuous stream of dielectric liquid used in actuators or for thermal management.<sup>[4]</sup>

Electro-fluidic actuators can be classified as follows: 1) capacitive electro-fluidic actuators and 2) resistive EHD actuators. Capacitive actuators use a compliant capacitor configuration: electrical forces between charges deform the system into a new equilibrium configuration, which depends on the applied voltage. Under a DC field, charges do not flow (except for leakage cur-

rents). AC driving is required for continuous power generation. Dielectric actuators, such as HASELS and HAXELS, zipping electro-ribbons, and devices based on dielectrophoresis and electro-wetting are all capacitive electro-fluidic actuators.<sup>[1-3,5]</sup> On the contrary, resistive EHD actuators generate power through a continuous flow of charges.<sup>[6]</sup> Electrodes pairs are exposed to the dielectric liquid. Ions are formed and discharged at the electrodes, creating a continuous flow of charges. They work under DC fields. Examples are ECF actuators, EHD conduction, and injection pumps, including recently developed EHD stretchable pumps.<sup>[4,7]</sup> In a previous work, the authors reported a configuration where one of the two electrodes in a pair is free to move, attached to a floating robot, whereas the other is fixed to the liquid container.<sup>[8]</sup> Wireless propulsion of the robot is enabled by using a layer of conductive liquid as electrical connection. Similarly, Chang et al. reported electro-osmosis as a propulsion method for miniature diodes.<sup>[9]</sup> By applying an AC field to a conductive solution, electro-osmotic flow is generated at the interface between each diode and the water, producing forces that displace or rotate the diodes. In this article, we move a step forward in wireless actuators for floating robots using EHD. We present a configuration where a floating robot is not only propelled but also positioned and stabilized by means of resistive EHD forces (Figure 1a).


## 1. Introduction

Electro-fluidic actuators use hydraulic coupling to transfer electrical forces. These actuators have high energy density and low power consumption, are compact, silent, and extremely versatile,

Prof. H. Shigemune, K. Pradidarcheep, Y. Kuwajima, Y. Seki, Prof. S. Maeda

Shibaura Institute of Technology  
3-7-5 Toyosu, Koto-ku, Tokyo 135-0061, Japan  
E-mail: hshige@shibaura-it.ac.jp

Dr. V. Cacucciolo  
Soft Transducers Laboratory (LMTS)  
École polytechnique fédérale de Lausanne (EPFL)  
rue de la Maladière 71b, CP 526, CH-2002 Neuchâtel, Switzerland  
E-mail: vito.cacucciolo@epfl.ch

 The ORCID identification number(s) for the author(s) of this article can be found under <https://doi.org/10.1002/aisy.202100004>.

© 2021 The Authors. Advanced Intelligent Systems published by Wiley-VCH GmbH. This is an open access article under the terms of the Creative Commons Attribution License, which permits use, distribution and reproduction in any medium, provided the original work is properly cited.

DOI: 10.1002/aisy.202100004

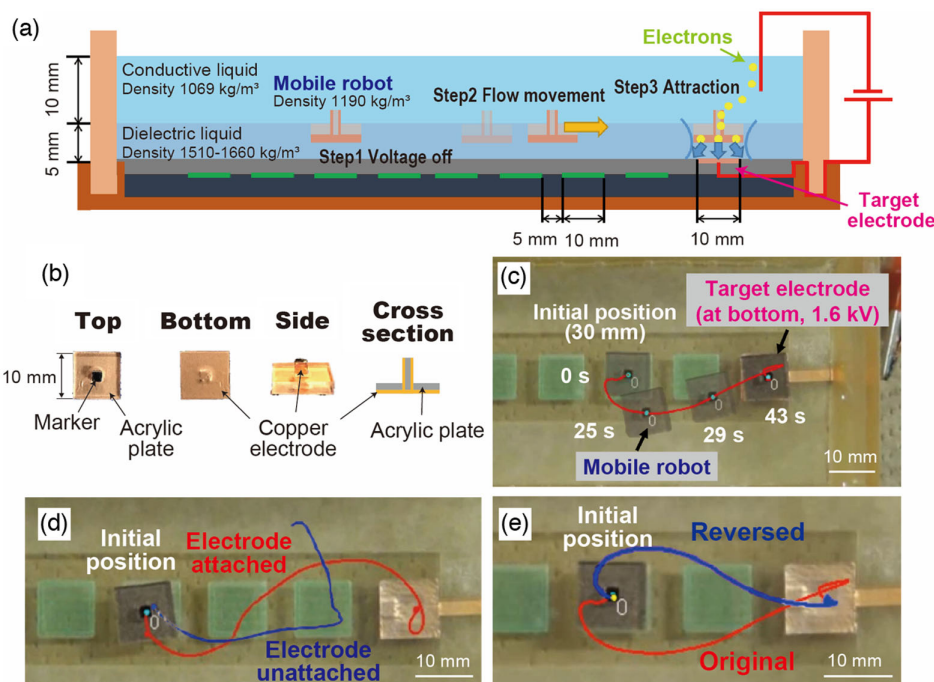


**Figure 1.** a) Schematics of the system. The mobile robot floats at the liquid–liquid interface between the top conductive liquid (density  $1070 \text{ kg m}^{-3}$ ) and the bottom dielectric liquid (density  $1510 - 1660 \text{ kg m}^{-3}$ ). The top conductive liquid is wired to the power supply and provides wireless electrical power to the robot. b) The simple robot is made of a laser-cut acrylic plate with a copper tape electrode attached. The electrode is exposed to the dielectric liquid and connected to the top conductive liquid. c) Top view of the setup in action. The initial position of the robot is 30 mm apart from the target electrode. When the voltage is turned on, the robot moves on to the target electrode following a curvilinear trajectory. d) The device is propelled and attracted onto the bottom electrode when the copper is attached (red trajectory). Without the copper, the propulsion still happens, but the attraction vanishes (blue trajectory) (Supplementary Video S3, Supporting Information). e) The robot follows different trajectories by changing the polarity of the applied voltage (Supplementary Video S4, Supporting Information).

In digital microfluidics, researchers use electro-fluidic actuators to move liquid droplets on arrays of electrodes through electrowetting.<sup>[10,11]</sup> Wireless powering and control of miniaturized robots has been demonstrated using magnetic fields.<sup>[12–15]</sup> Recent efforts demonstrated the deformation of soft-bodied robots, built by dispersing magnetic powders into elastomers.<sup>[16,17]</sup> However, magnetic actuators require large, expensive electromagnets and high electrical currents ( $\approx 10 \text{ A}$ ), leading to complex, high-cost, and energy-hungry systems.<sup>[13]</sup>

Acoustic fields can also be used to move and position objects wirelessly. Acoustic levitation offers high precision and freedom in selecting the object's materials, but still requires a large number of ultrasonic transducers and generates low forces.<sup>[18]</sup>

The actuators presented in this work rely on resistive EHD and are based on a simple, compact hardware (Figure 1), which requires very low power ( $< 1 \text{ mW}$ ) to operate. EHD actuators include a wide variety of mechanisms, including charge injection, conduction pumping, electrowetting, and the Onsager effect.<sup>[6,19]</sup> The actuators reported in this work are based on charge injection EHD. The setup includes two vertically stratified liquids in a container: one dielectric on the bottom and one conductive on the top (Figure 1a). The buoyancy of the robot is designed for floating at the interface between the two liquids. The robot has an attached electrode, which is both electrically connected to the top conductive liquid and exposed to the bottom

dielectric liquid. Target electrodes (sized  $10 \text{ mm} \times 10 \text{ mm}$ ) are attached to the bottom of the liquid container.

Using a similar configuration (resistive EHD, stratified liquids), the authors reported in a previous work the wireless propulsion of a robot.<sup>[8]</sup> In this article, we demonstrate for the first time that such propulsion exists not only when the robot is over the bottom electrode but also when the robot is distant from it. We also report that the robot always moves toward the addressed bottom electrode, until reaching it and stopping there in a stable position.

We measured electrical currents below  $1 \mu\text{A}$ ,  $10^6$  times smaller than in magnetic-driven systems. Although voltages are higher for EHD compared to electromagnetic actuators ( $10^3$  vs  $10^0 \text{ V}$ ), power consumption is still 1000 lower for EHD actuators ( $10^{-3}$  vs  $10^0 \text{ W}$ ).

We characterize the motion of the robot for different values of the applied voltage and different dielectric liquids. We also show how the trajectory followed by the robot moving toward the target electrode changes by changing the polarity of the applied voltage. We further investigate the underlying mechanism, pondering the relative contributions of resistive EHD forces and capacitive electrical forces between the two electrodes. Finally, we demonstrate the system in action by controlling the trajectory of the robot through sequential activation of an array of target electrodes.

## 2. Results and Discussion

Figure 1a shows the schematics of the system. A mobile robot floats at the liquid–liquid interface between a conductive water solution (on top) and dielectric liquid (on bottom). As dielectric liquids, we tested two fluorinated hydrocarbons, Novec 7100 and Novec 7300. Suitable liquids for EHD are good electrical insulators (to allow high electric fields) and have low viscosity (to reduce the fluidic impedance). Detailed criteria for selecting EHD liquids are described in a patent by Yokota and colleagues.<sup>[20]</sup> We selected Novec 7100 and 7300 as their properties make them excellent EHD liquids (Figure S1, Supporting Information) and in addition they have low toxicity and are widely available. The actuators reported in this work can arguably work with other suitable EHD liquids as well.

An electrode is attached on the bottom face of the robot (Figure 1b). One side of this electrode is exposed to the dielectric liquid, the other side is connected to the top conductive liquid, providing wireless electrical connection to the power supply. A second electrode, called target electrode, is attached to the bottom of the container. Applying a voltage between the conductive liquid and the target electrode induces an electric field in the dielectric liquid. As the voltage overcomes a threshold of 400 V, the dielectric liquid gets ionized by charge injection in the proximity of the negatively charged electrode. The ions being formed are subject to electrophoretic forces generated by the charges on the electrodes. These forces make the ions travel from the negatively charged to the positively charged electrode, where they discharge. The motion of ions generates fluid circulation and the deformation of the liquid–liquid interface. (Figure S2 and Supplementary Video S1, Supporting Information). For the action–reaction principle, opposite forces are generated on the charges on the electrodes, including the electrode attached on the robot. A combination of fluid circulation and reaction forces propels the robot from its initial position on to the top of the target electrode. The robot covers a gap of 30 mm in 43 s, at an applied voltage of 1.6 kV (Figure 1c). In addition to propulsion, these EHD forces position and stabilize the robot over the target electrode. Figure 1d plots the trajectories of the center of the robot with and without an electrode attached to it. When an electrode is attached (red curve), the robot is propelled and stabilized over the target electrode. When the electrode is not attached (blue curve), the robot is still propelled, but the attraction vanishes (Supplementary Video S3, Supporting Information). Figure 1e shows the different trajectories followed by the center of the robot when the polarity of the applied voltage is reversed compared to the experiment in Figure 1d. The red curve corresponds to positive voltage applied to the target electrode and ground connected to the top conductive liquid. The blue curve corresponds to reverse connection (Supplementary Video S4, Supporting Information).

Figure 2a shows the container with a size of 150 mm × 51 mm × 30 mm that we used for the characterization experiments. The robot initial positions respect to the target electrode are marked with green tape: D1 = 15 mm, D2 = 30 mm, D3 = 45 mm, D4 = 60 mm, and D5 = 75 mm. Figure 2b plots *x* position over time for the mobile electrode starting at initial positions D1 to D5. It takes 46 s to reach the target electrode from position D5 = 75 mm. The plot also shows the stabilization dynamics

of the robot over the target. Figure 2c summarizes the reaching time starting from different initial positions. The data show a quadratic correlation between time and initial distance. Figure 2d plots distance versus time using different dielectric liquids and voltage values. The initial position is D3 = 45 mm. We applied 1.2–1.6 kV for Novec 7300, and 1.2–1.4 kV for Novec 7100, since at 1.6 kV Novec 7100 presents electrical breakdown. The reaching time decreases by increasing the voltage and is always shorter for Novec 7100 than for Novec 7300, arguably due to lower viscosity and higher permittivity of Novec 7100 compared to Novec 7300 (Figure S1, Supporting Information).<sup>[21]</sup>

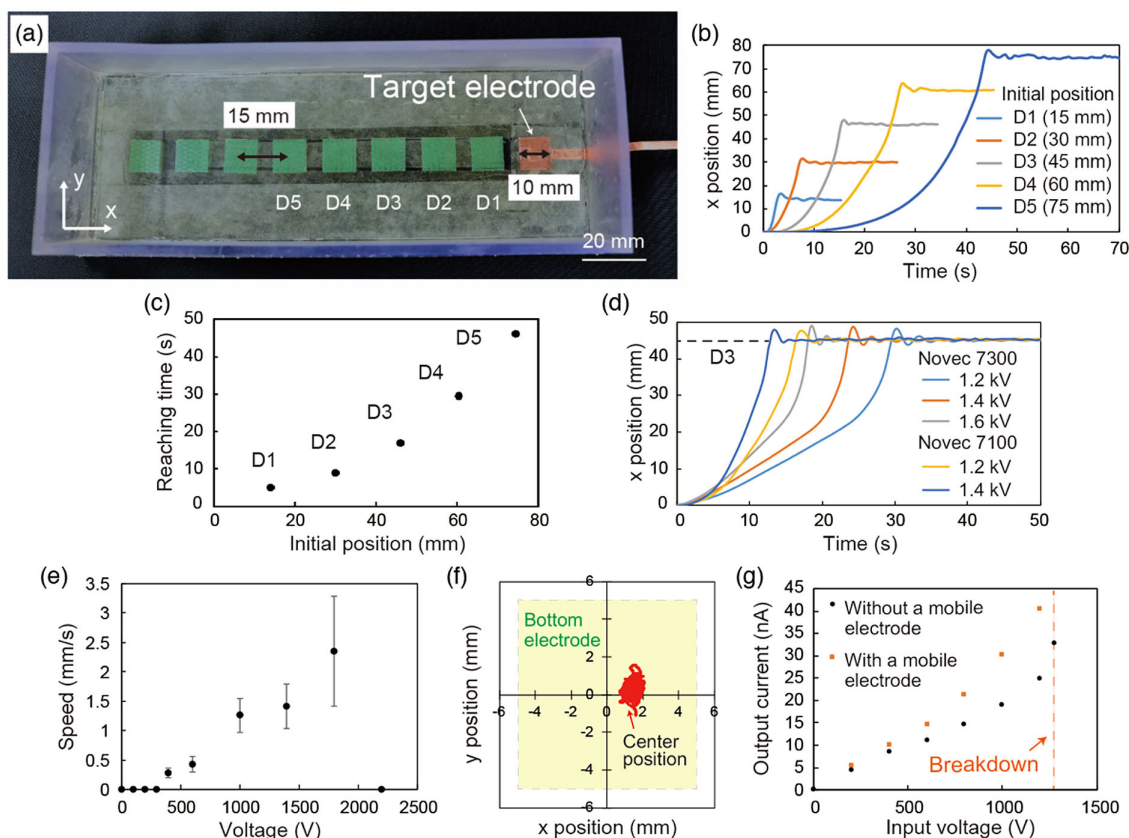
Figure 2e plots the average speed of the mobile electrode for different applied voltages. As expected, higher voltage leads to higher speed. For each voltage value, the speed is calculated as the average of distance divided by time, over four trials, each having the mobile robot starting from a different initial position. With Novec 7300, the minimum voltage to observe robot motion is 400 V, whereas the maximum voltage before electrical breakdown is 1.8 kV. A 400 V is a relatively low voltage for electrostatic actuators and, with low-power consumption, can be generated by subgram electronics, enabling compact and portable systems.<sup>[22]</sup> The driving voltage can be further reduced by decreasing the height of the dielectric liquid.

Figure 2f shows an experiment to evaluate the stability of the attraction between the robot and the target electrode. We tracked the position of the center of the robot for a time of 50 s, finding that it lies within a circle of 1.5 mm radius positioned over the target electrode.

Figure 2g plots the electrical current flowing in the system for different values of the applied voltage. During this experiment, the robot is positioned over the target electrode. The extremely low values (<50 nA) confirm the low power consumption to keep the robot position (<0.05 mW). The current is calculated by measuring the voltage drop in a 1 MΩ shunt resistor connected in series with the system. As a comparison, we measured the electrical current also without the mobile electrode, obtaining even lower values.

We conducted a qualitative experiment to assess the relative contributions of resistive EHD and capacitive electrostatic attraction in the force driving the robot. We covered the target electrode with a thin Kapton tape (25 μm polyimide film and 40 μm silicone adhesive). The presence of the insulation on one of the two electrodes is expected to nullify resistive EHD forces, which rely on ion injection and discharging of ions in contact with the electrodes. Capacitive electrostatic attraction depends mostly on electric field and dielectric constant. As a consequence, it is not significantly affected by the presence of the insulating tape, given the low thickness of the tape compared to the gap between the electrodes (65 μm vs 5 mm) and similar dielectric constants (3 for tape and 7 for liquid). With voltages up to 3.5 kV, we qualitatively observed that the attraction toward the target electrode vanished completely with Kapton tape insulation (Figure S3, Supporting Information), confirming the dominant role of resistive EHD forces in this system.

We demonstrate the ability to control the trajectory of the miniaturized robot by sequential activation of a series of target electrodes (Figure 3 and Supplementary Movie S5, Supporting Information). Figure 3 (top) shows the schematics of the experiment. The robot is tested in a squared container with an array of



**Figure 2.** Experimental setup and results. a) Top view of the container with the different green square markers representing the initial positions D1 to D5 of the robot during the experiment. The distance between the centers of two adjacent markers is 15 mm. b) Time evolution of the x position of the center of the robot starting from different initial positions. Voltage is applied at time zero. c) Plot of reaching time starting from different initial positions. The more-than-linear correlation results from the EHD driving force being inversely proportional to the distance squared. d) Displacement in time of the mobile electrode with different values of the applied voltage and different dielectric liquids. The reaching time is lower with Novec 7100, having lower viscosity and higher permittivity, even at lower voltage. Data in graphs (b–d) acquired with motion analysis at 15 Hz and plotted without further processing. e) Average speed of the robot for different values of applied voltage. Liquid is Novec 7300. The minimum voltage to drive the robot is 400 V. The dot at 2200 V (zero speed) represents an electrical breakdown. Data points represent average over four trials and error bars represent standard deviation. f) Trajectory of the center of the mobile robot while on the target electrodes, in 50 s time with voltage applied. g) Electrical current by varying the voltage, with and without the mobile robot.

3 × 3 target electrodes attached on the bottom. We activate one electrode at-a-time in predefined sequences to draw trajectories correspondent to the letters I, S, and T. The robot is always electrically connected to the ground through the top conductive liquid. The robot follows the defined trajectory, always moving toward the addressed electrode. The stability and accuracy of the positioning is influenced by the flow of liquid in the container. Reducing the size and increasing the number of electrodes will enable more accurate control of the path of the robot.

### 3. Conclusion

In conclusion, we propose a novel approach to wirelessly propel and position floating mini robots using resistive EHD at the interface between two stratified liquids. Advantages of this approach compared to the use of magnetic or acoustic fields include the use of simple DC electric fields with thin, flat

electrodes, without complex wiring and electronics, low current and low power consumption, powering, and stable positioning with just one signal. We demonstrated the proposed concept using a simple mobile floating robot. We characterized the performance of the system in terms of response time, workspace, speed, current, and power consumption. We finally demonstrated the trajectory control of the robot by sequential activation of an array of target electrodes.

This work is a first proof of concept for the use of resistive EHD for the wireless powering and positioning of mobile robots. Integration and scalability drawbacks need to be addressed before using this system in application scenarios. The current configuration can only work on a horizontal plane due to the stratified conductive and dielectric liquid. Electrodes degradation and stability over time needs to be evaluated. Future developments include the miniaturization of the robot, the use of denser arrays of target electrodes driven by compact multichannel electronics, and including embedded sensors and computation.



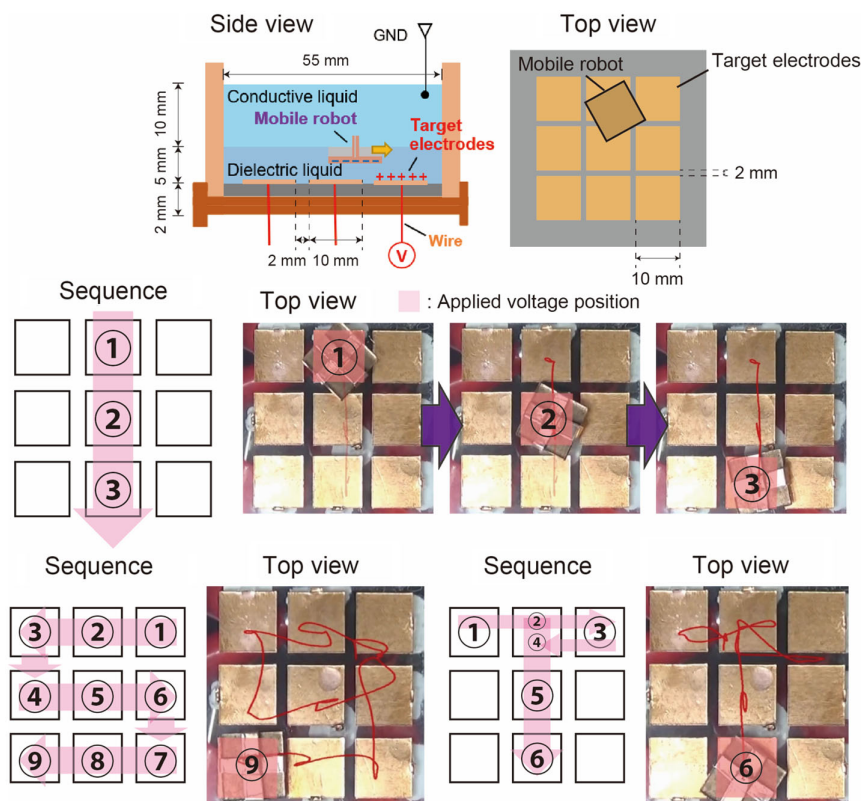


**Figure 3.** Demonstration of trajectory control with the mobile robot. Top schematics show the top view and side view of the system. The 3 × 3 squared target electrodes with 10 mm side each are attached at the bottom of a squared container. By addressing the target electrodes in series, the robot motion follows an I, an S, and a T trajectory (red lines).

One can imagine multiple robots that collaborate in complex tasks, coordinated by a central unit or acting based on local robot–robot interactions. The extreme simplicity of our wireless EHD actuators compared to electromagnetic and acoustic technologies makes it a good candidate for application in soft machines. Acrylic plastic and copper electrodes can be replaced by elastomers and conductive elastomers (i.e., a mixture of elastomer and conductive particles) without affecting the functionality of the system. The applications of this technology are broad and include precision assembling at the micro/mesoscale, lab-on-chip, tactile displays, and active surfaces.

## 4. Experimental Section

**Fabrication of Liquid Container:** The rectangular container had internal dimensions of 150 × 51 × 30 mm. The frame and base were fabricated using a 3D printer (Form 2, formlabs). The conductive liquid was an aqueous solution of sodium chloride, 1.7 M.

**Mobile Robot:** Figure 1b consists of a hull made of a laser-cut acrylic plate, an electrode made of copper tape bonded to the bottom of the hull, and with a side in contact with the conductive liquid on top.

**Dielectric Liquids:** Novec 7100 and Novec 7300 were purchased by Hayashi Rikagaku Corp. and used without additional treatment.

**Power Supply:** HEOPT-20B10 produced by MATSUSADA Precision Corp.

## Supporting Information

Supporting Information is available from the Wiley Online Library or from the author.

## Acknowledgements

The authors thank the Japan Society for the Promotion of Science for their support under Grants-in-Aid for Scientific Research programs Grant-in-Aid for Scientific Research on Innovative Areas (Research in a proposed research area) 18H05473, Grant-in-Aid for Challenging Exploratory Research 16H04306, 19K21950, and Early-Career Scientists 19K20377. *The Interactive Supporting Information of the article can be found at:* <https://authorea.com/doi/full/10.22541/au.161471084.45799146/v1>.

## Conflict of Interest

The authors declare no conflict of interest.

## Data Availability Statement

Research data are not shared.

## Keywords

electrohydrodynamics, liquid electrodes, positioning, wireless actuators

Received: February 1, 2021

Revised: March 28, 2021

Published online: May 14, 2021

- 
- [1] S. K. Mitchell, X. Wang, E. Acome, T. Martin, K. Ly, N. Kellaris, V. G. Venkata, C. Keplinger, *Adv. Sci.*, **2019**, 6, 14.
- [2] E. Leroy, R. Hinchet, H. Shea, *Adv. Mater.* **2020**, 2002564.
- [3] M. Taghavi, T. Helps, J. Rossiter, *Sci. Robot.* **2018**, 3, eaau9795.
- [4] V. Cacucciolo, J. Shintake, Y. Kuwajima, S. Maeda, D. Floreano, H. Shea, *Nature* **2019**, 572, 516.
- [5] T. B. Jones, *Langmuir* **2002**, 18, 4437.
- [6] A. Ramos, *Electrokinetics and Electrohydrodynamics in Microsystems*, Springer, Vienna, **2011**.
- [7] T. Nagaoka, Z. Mao, K. Takemura, S. Yokota, J.-w. Kim, *Smart Mater. Struct.* **2018**, 28, 025032.
- [8] V. Cacucciolo, H. Shigemune, M. Cianchetti, C. Laschi, S. Maeda, *Adv. Sci.* **2017**, 1600495.
- [9] S. T. Chang, V. N. Paunov, D. N. Petsev, O. D. Velev, *Nat. Mater.* **2007**, 6, 235.
- [10] M. G. Pollack, R. B. Fair, A. D. Shenderov, *Appl. Phys. Lett.* **2000**, 77, 1725.
- [11] M. Abdelgawad, A. R. Wheeler, *Adv. Mater.* **2009**, 21, 920.
- [12] T. Inoue, K. Iwatani, I. Shimoyama, H. Miura, in *IEEE Int. Conf. on Robotics and Automation (ICRA)*, IEEE, Piscataway, NJ **1995**, p. 678.
- [13] S. Miyashita, S. Guitron, S. Li, D. Rus, *Sci. Robot.* **2017**, 2, eaao4369.
- [14] X. Li, Q. Shi, H. Wang, T. Sun, Q. Huang, T. Fukuda, *J. Micromech. Microeng.* **2017**, 27, 125014.
- [15] A. Barbot, H. Tan, M. Power, F. Seichepine, G. Z. Yang, *Sci. Robot.* **2019**, 4.
- [16] Y. Kim, H. Yuk, R. Zhao, S. A. Chester, X. Zhao, *Nature* **2018**, 558, 274.
- [17] W. Hu, G. Z. Lum, M. Mastrangeli, M. Sitti, *Nature* **2018**, 554, 81.
- [18] Y. Ochiai, T. Hoshi, J. Rekimoto, *ACM Trans. Graphics* **2014**, 33, 85.
- [19] J. C. Ryu, H. J. Park, J. K. Park, K. H. Kang, *Phys. Rev. Lett.* **2010**, 104, 104502.
- [20] S. Yokota, Y. Otsubo, K. Edamura, US6030544A. **2000**
- [21] Y. Kuwajima, H. Shigemune, V. Cacucciolo, M. Cianchetti, C. Laschi, S. Maeda, in *2017 IEEE/RSJ Int. Conf. on Intelligent Robots and Systems (IROS)*, IEEE, Piscataway, NJ **2017**, p. 470.
- [22] X. Jin, X. Liu, V. Cacucciolo, M. Imboden, Y. Civet, A. E. Haitami, S. Cantin, Y. Perriard, H. Shea, *Sci. Robot.* **2019**, 4.